Journal of Basic and Bio Sciences
An International Journal

http://dx.doi.org/01.2024/jb2s/0101

Modulation of the rate of electron transfer in the redox reaction of an octahedral Co(III) complex in reverse micellar milieu and presence of salts in ionic micelles

Mousumi Mukherjee

Department of Chemistry, Khalisani Mahavidyalaya, Chandannagar, Hooghly, India

Received: 10th November, 2024, Revised:20th November, 2024 , Accepted: 5th December, 2024.
Published online: 7th December, 2024.

Abstract: *Electron transfer reactions have beneficial implications from biological applications to industrial relevance. Several transition metal complexes have been used as model systems for studying electron transfer reactions. We have picked the octahedral Co(III) complexes from among them due to their inert characteristic making them ideal for theoretical and experimental studies. Kinetics of reduction of Co(III) complexes is negligibly affected by reversible electron transfer, incorporation of water molecules, substitution and isomerisation reactions. Herein, such studies have been performed on the reduction of pentamminechlorocobalt(III) nitrate, [Co(NH3)5Br](NO3)2 by Mohr's (Fe(II)) salt. Effect of ionic micelles on the redox reaction was studied spectrophotometrically and the influence of various soluble salt concentrations on the reaction rate has been monitored. The outcome of the effect of the water pools of anionic reverse micelles of SDS/1-butanol/n-heptane was also monitored and the results were intriguing. The redox reaction in aqueous solution has been parallelly investigated using a theoretical quantum mechanical approach. The analyses of structures of the reactants, transition state, products and calculation of their energies were done using the density functional theory (DFT). The calculated energy values corroborate with the experimental ones. The activation energies were calculated at three levels of ab initio molecular orbital theory [HF, DFT (B3LYP) and MP2] combined with three basis sets (3-21G*, 6-31G* and 6-31+G**).*

Keywords: Electron transfer, redox reaction, octahedral Co(III) complex, transition state, inner sphere mechanism

1. Introduction

In the past two decades, the importance of organized assemblies on biological, photophysical and kinetic processes has been accepted globally. Reactants accommodated in molecular assemblies such as micelles, micro-emulsions and vesicles, etc., often achieve a greater degree of organization in homogeneous continuous solution and can mimic reactions in bio-systems, and also have potentials for energy storage [1-6]. The behavior of a molecule at an interface between two bulk media is often significantly different from that in either of them. Since the polarity and viscosity at the interface are often very much different from those of the bulk media, the structure, dynamics and reactivity of an organic or bio-molecule at an interface differ noticeably from those observed in the bulk. Interestingly most natural and biological processes occur at such interfaces or in confined systems, e.g., proteins, bio-membranes and vesicles. Typical example of such membrane mimetic model is "reverse micelle", which is an organized assembly of surfactant in continuous organic solvent. Study of reverse micellar environments is of growing importance and is recognized as a method to better understand the mechanisms involved, as well as a route to control the rate and to improve reaction yields. It has been reported that water pools in reverse micellar cavities have a much lower micro-polarity than the bulk phase, which can influence kinetic features [7-9]. Interactions between the substrate and the polar head groups of the surfactant, between the substrate and the solubilized water and between the solubilized water and the surfactants can be intense and definite. Here we have reported the rate of reduction of pentamminechlorocobalt(III) nitrate, $[Co(NH_3)_5Br](NO_3)_2$ by Mohr's (Fe(II)) salt in SDS reverse micellar systems. Besides this, several additives, e.g., salt and urea in presence of surfactant can also alter the rate of the reaction as polarity of the medium changes [10,11].

We have chosen such inner sphere reactions to determine the activation energy experimentally and compared the results theoretically by density functional theory (DFT)and Hartree-Fock (HF) methods. However, in order to reproduce the experimental values of the activation energy, it is necessary to employ *ab initio* methods and a good

*Corresponding author e-mail: mukherjee88@gmail.com

basis set [12,13]. The most demanding computational analysis is evaluation of activation barrier for chemical reaction. Thus, we prefer to calculate the activation energy of the reaction.

The applicability of the DFT dealings for estimating various thermochemical properties is an area of continuing research interest [14-17]. There are some advantages in using the DFT procedure. Firstly, it is computationally inexpensive compared to the high level *ab initio* methods based on molecular orbital theory and thus calculations can be performed with a large basis set. Moreover, DFT methods scale much more favorable with the size of basis set [18,19]. With this in mind, we report the accurate energies computed from the combination of three levels of theory: Hatree-Fock (HF), second order Møllet-Plesset (MP2) [20] and the density functional B3LYP scheme [21,22], and three popular basis sets, 3-21G*, 6-31G* and 6-31+G** [23] in DFT level and LanL2DZ basis set for the electron core potential (ECP) calculations in the HF level.

2. Experimental

2.1 *Materials and methods* All the reagents used were of either GR or AR grade. Sodium dodecyl sulphate (SDS), potassium chloride (KCl), potassium nitrate (KNO_3), potassium sulphate (K_2SO_4), potassium perchlorate ($KClO_4$), urea, Mohr's salt, ammonium sulphate, sulphuric acid, 1-butanol and n-heptane were used as obtained from Merck (India). N-cetyl-N, N, N-trimethyl ammonium bromide (CTAB) of 98% purity from Loba Chemie (India), from SRL India were used as received. All aqueous solutions were prepared in deionised and double distilled water with second distillation being carried out from alkaline permanganate in all Pyrex still.

The $[Co(NH_3)_5Br](NO_3)_2$ complex was prepared by a standard method [24].This coordination compound was characterized long back in 1962 by Shimanouchi and Nakagawa [25] and later analyzed by Watt and Klett [26] and Jordan et al. [27]. The metal-ligand stretching and skeletal deformation frequencies for the cobalt pentammine complex were expected [25]. Therefore, the skeletal frequencies are hardly affected by ligand frequencies and in the analysis of skeletal frequencies. The NH_3 ligand vibrations were assigned in the IR spectrum, where the lowest one of these is due to the NH_3 rocking vibration observed near 800 cm^{-1}. The molecular symmetry of $[Co(NH_3)_5X]^{2+}$is assumed to be C_{4v}. In these ions the vibrations of the A_1 and E-species were found to be infrared active among which some remain invisible due to weak intensity because of the nature of their vibrational modes [25].The Co-Br stretching in $[Co(NH_3)_5Br](NO_3)_2$ is observed at 487 cm^{-1} [26].The compound that we have used was obtained as gift from Prof. C.R. Sinha of Jadavpur University in pure form and hence we checked its UV spectrum to ensure the purity (Fig. 1).

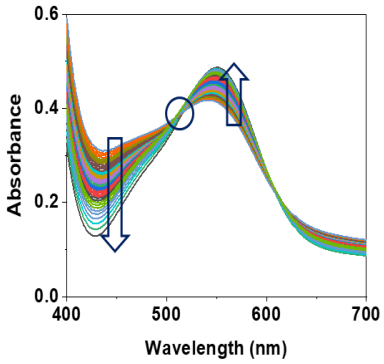

Figure 1

All kinetic and spectral measurements were recorded on Agilent 8453E UV-visible spectroscopy system. Quartz cells (1.0 cm optical path length) from Hellma were used.The kinetic studies of the reaction between $[Co(NH_3)_5Br](NO_3)_2$ and Mohr's salt in different micro heterogeneous media were studied spectrophotometrically at 298 K. Concentrations of reactants were chosen such that iron(II) was always in considerable excess, which was often sufficient (≥ 40 times) to ensure pseudo first order condition. All kinetic runs were performed at 298 K by

mixing required volumes of the thermostated reactants with proper dilution to the required volume in the quartz cell. The change proceeds through an isosbestic point at ca. 507 nm with a decrease in absorbance at ca. 550 nm and an increase at ca. 425 nm (Fig. 1). The decrease in absorbance (A_t) of the reaction mixture with time(s) was recorded at 550 nm. The integrated rate equation used to determine the observed pseudo first order rate constant, k_{obs} values from the plot is: $A_t = A_\infty + a_1 exp(-k_{obs} \times t)$; which is first order exponential decay equation. The standard error in determination of k_{obs} value was within ±3%.

3. Computational details

All the computations were performed with the GAUSSIAN 03 (G03) program suite [28]. Both ground and transition state geometries were fully optimized in aqueous medium at DFT (B3LYP) levels (the Becke's three-parameter hybrid exchange [29] with the Lee-Parr-Yang correlation functional) [30] with Pople's 6-31G* basis set [31],and LanL2DZ basis sets, used to calculated the core electron potential, are internally available in the Gaussian package which is a multi-processor system.Frequency calculations were also carried out for ground and transition state geometries and it is observed that the latter having one imaginary frequency corresponding to the reaction coordinate. The activation energy in this study was calculated as the energy difference of the sum of total energy, plus zero-point energy (calculated in the consistent level) and the thermal energy at 298K between the reactant and transition state structure and the value compares/agrees very well with the experimentally determined value.

4. Results and discussion

4.1 *Kinetic effects*

The Fe^{II} salt (Mohr's salt) reduces $[Co(NH_3)_5Br]^{2+}$following second order kinetics as shown below [32]:

$$[Co(NH_3)_5Br]^{2+} + Fe^{2+} + 5H^+ = Co^{2+} + Fe^{3+} + Br^- + 5NH_4^+ \quad (1)$$

Here, the relative effect of aquation (eqn. 2) is minimized at high Fe^{II} concentration.

$$[Co(NH_3)_5Br]^{2+} + H_2O = [Co(NH_3)_5(H_2O)]^{3+} + Br^- \quad (2)$$

Formation of the bimolecular bromo-bridged inner sphere complex permits transfer of an electron from Fe^{II} to Co^{III} involving a bridged complex with both metals in octahedral centers [33].The halide ligand as electron mediator in this process where the higher polarisability of the heavier halide ions are more effective. The reaction is first order with respect to both the Co^{III} complex and Fe^{II} salt.

$$-\frac{d[Co^{III}]}{dt} = k[Co^{III}][Fe^{II}]$$

4.2 *The effect of reverse micelles on the reaction*

The hydrophobic heads of the surfactants are exposed to the surrounding non-polar solvent molecules in a reverse micelle, which is energetically unfavourable, and gives rise to a water-in-oil system. The hydrophilic groups are sequestered in the micelle core and the hydrophobic groups extend away from the centre. Inverse micelles are proportionally less likely to form on increasing head group charge, since hydrophilic sequestration would create highly unfavourable electrostatic interactions [34]. The alkenes, iso-octane or n-heptane, permit maximum solubilization of water at room temperature and thus are normally used to stabilize the reverse micelle. Increase in the amount of surfactant-entrapped water results in the formation of water-in-oil microemulsions. Effect of varying the concentration of SDS on the reaction rate has been studied at different values of W (4 - 10) (defining the concentration of water in the microemulsions and hence the aqueous pool size)as shown in Fig. 2. The reverse micelles of SDS (0.10 - 0.30 $molL^{-1}$) have significant effect on the rate of the reaction at lower W value. The reactants being ionic cannot exist in the bulk organic phase; thus the reaction takes place either within the water pool entrapment or in the micellar interphase. It is known [38] that at constant W the increase in surfactant concentration results in increase of the micellar concentration and hence the area of the interface, with no change of the micellar composition and other properties [35].

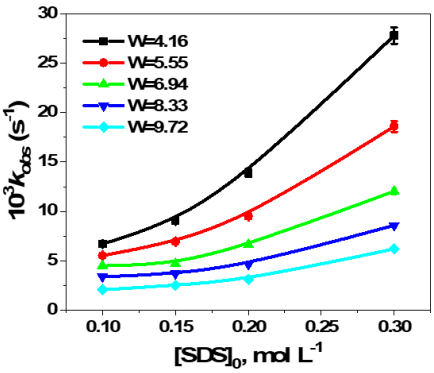

Fig. 2

Thus, increase of rate with SDS concentration shows that the reaction is taking place on the micellar interface at low W value. At high value of W the effect of SDS concentration is much smaller. The increase in the surfactant concentration at high W value increases the interfacial area and thus the reactants are displaced from the micellar interface to the bulk of large sized water pool. Hence, the reaction takes place mainly in the bulk of the entrapped water pool [36]. Thus, at high W value the reverse micelle has very little effect on the rate. In other words, as W increases, the properties of the entrapped water pool become similar to those of bulk water.

It has been found that the rate of reaction in presence of SDS reverse micelles is much higher than that in presence of TX-100 [37]. This is because the substrates are attracted towards the SDS surfactants with higher coulombic force of attraction than that of the TX-100ones. Anionic surfactants help to increase the probability of encounter between the Co^{III} complex and Mohr's salt through interaction between the compact region of the charged head groups and the relatively small counters ions. Thus, rate of the reaction in presence of TX-100 reverse micelles is lower compared to SDS due to the low encounter probability between the Co^{III} complex and Mohr's salt.

4.3 *Effect of urea and salts on the reaction in micellar medium*

Micellar catalysis is affected in the presence of additives, such as urea, $KClO_4$, KNO_3, K_2SO_4 and KCl (Fig. 3(a) and3(b)). The rate of reduction diminishes upon addition of 8 $mmolL^{-1}$ urea to the aqueous solution of CTAB above its CMC (10^{-3} $molL^{-1}$). The rate of electron transfer (and hence reduction) was also determined in presence of SDS.The CMC values of CTAB and SDS are well known and hence we have considered them as reported. Most likely, urea decreases the polarity of the aqueous phase affecting the stability of the transition state, and hence lowering the rate of the ionic reaction. However, addition of KCl increases the reduction rate. KCl increases polarity of the medium, enhancing the rate of the reaction since the transition state is supposed to be positively charged. So is the case with other added salts where the rate of the reaction increases due to increase in the polarity of the medium.

All the above results indicate a vital role of the non-ccoulombic interactions in accelerating the rate of reduction of the Co^{III} complex in micellar medium [37]. Due to the non-coulombic interaction, the surfactants form micelles of colloidal size [38] and occupy large space in the reaction volume ultimately increase the local concentration of the reacting species as well as the rate. Non-coulombic interaction persists due to the hydrophilic nature of the Co^{III}complex [39]. The non-coulombic interaction gains more importance for the SDS micelles over the CTAB ones because of coulombic repulsions [40].The cationic complex binds to the SDS micelles by coulombic as well as non-coulombic interactions. The stronger force of attraction between the negatively charged SDS micelles and the complex induces a degree of immobilization to it and explains qualitatively its faster rate of reduction in presence of salts. The reduction rate does not increase appreciably in the cationic micelles due to the low collision probability between the complex and the Mohr's salt.

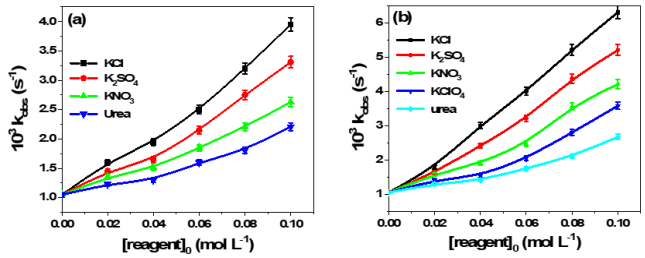

Fig. 3

4.4 *Calculation of activation energy by DFT*

The calculated activation energies(E_a) obtained at different levels are given in Tables1and2at 298 K.The E_a values were calculated from the Arrhenius equation ($k = Ae^{-E_a/RT}$), where k= the rate constant, A= pre-exponential factor, E_a= activation energy, R= universal gas constant and T= temperature in kelvin.The second column of Table 2shows the differences between the calculated and experimental activation energyy and the last column contains the total time for computing that includes the optimization time for reactants and transition states. The following observations are apparent from here.

(i) The DFT method produces the highest calculated activation energies which are closer to the experimental values; whereas those calculated from MP2 and HF are lower. It is logical that the density functional scheme produces better results than the single HF Hamiltonian. However, the HF LanL2DZ basis set, which includes the electron core potential, provides satisfactory values.

(ii) The activation energies obtained from the MP2 scheme are similar to those obtained with the HF method.

(iii) However, with basis sets of moderate size, 6-31G* and 6-31+G*, the results are better with the DFT method. The small basis set 3-21G* produces lower values than the other two basis sets.

(iv) Results from 6-31G* and 6-31+G* basis sets are similar. This is a consequence of the analogy of the two last basis sets despite the differences in computational time. For this reason, it is better to use the quick and economical basis set 6-31G* instead of the slow and expensive 6-31+G*.

(v)The best calculated activation energy was obtained from the combination B3LYP/6-31G*, but the activation energy calculated with the combination B3LYP/6-31+G* is almost as good. The use of the expensive basis set 6-31+G* is unnecessary for this type of calculation.

(vi) As indicated in the last column of Table 2, whatever the method utilized, the basis set 6-31+G* requires the longest computing time and hence looks impractical as is with MP2. Values obtained using the HF-LanL2DZ basis set are acceptable within appropriate error since it saves large calculation time.

Table 1. Activation energy (E_a) and standard enthalpy of activation ($\Delta^{\ddagger}H°$) for the reaction of $[Co(NH_3)_5Br](NO_3)_2$ and Mohr's salt in aqueous solution at 298 K.

Parameters	Calculated		Experimental	
	$kJmol^{-1}$	Method used	$kJmol^{-1}$	Method used
Activation energy (E_a)	76.78	B3LYP/6-31G*	76.29	Arrhenius plot
Standard enthalpy of activation ($\Delta^{\ddagger}H°$)	65.10	B3LYP/6-31G*	61.42	Eyring plot

Table 2 Activation energy (E_a) for the reaction of $[Co(NH_3)_5Br](NO_3)_2$ and Mohr's salt in aqueous solution at 298 K, E_a(exp) = 76.29 ($kJ\ mol^{-1}$).

Method	E_a(cal) (kJ mol^{-1})	E_a(cal) - E_a(exp) (kJ mol^{-1})	Time
HF/3–21G*	75.74	-0.55	2 h 35 min
HF/6–31G*	76.24	-0.05	3 h 5 min
HF/6–31+ G**	76.26	-0.03	3 h 55 min
B3LYP/3–21G*	76.17	-0.12	7 h 15 min
B3LYP/6–31+ G**	76.50	0.17	9 h 5 min
MP2/3–21G*	75.83	-0.46	8 h 20 min
MP2/6–31G*	76.23	-0.06	9 h 50 min
MP2/6–31 + G**	76.21	-0.08	11 h 10 min
HF/LanL2DZ	77.00	0.71	1 h 10 min

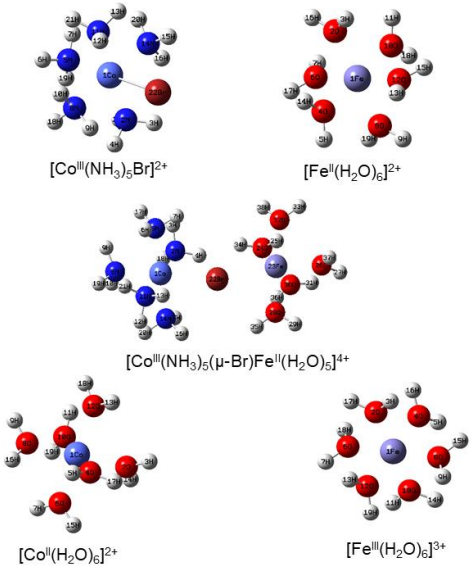

Scheme 1.

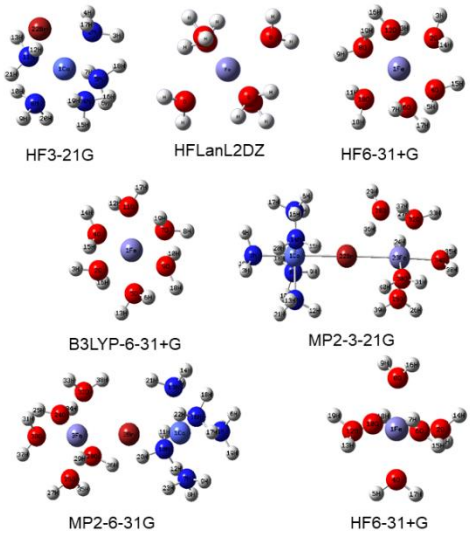

Scheme 2.

The different levels of calculations provide the optimized geometries of the reactant, product and transition state (Scheme 1 and 2). The calculated activation energies suggest that all the reactions proceed easily and the results agree with the experimental observations. However, the optimized geometries showed slight difference. Inner

sphere electron transfer proceeds via a covalent linkage between the two redox partners. Here the Br^- ligand bridges the two metal redox centers during the event of electron transfer. The energy of the transition state varies with the change of ligand. These reactions are inhibited by large ligands, which prevent the formation of the crucial bridged intermediate. Br^- ligand serves as an electron donor. Electron transfer occurs reversibly through the bridge once it is established through a transition state during the reaction.

Table 3. Equilibrium bond lengths and bond angles (of selected ones) of the reactants (R), transition state (TS) and products (P) using different basis set.

Parameter	Method	R		TS	P	
		Co^{III}	Fe^{II}		Co^{II}	Fe^{III}
Bond length (Å)	HF/3-21G*	3.76/ 2.92	2.01	2.30/ 4.60/ 2.63	2.57	1.82
	HF/6-31G*	4.08/ 2.88	2.07	4.30/ 7.08/ 2.86	2.57	1.93
	HF/6-31+G**	3.80/ 2.87	2.04	3.76/ 5.76/ 2.63	2.55	1.99
	B3LYP/3-21G*	4.98/ 2.90	2.00	2.29/ 4.29/ 3.42	2.57	1.94
	B3LYP/ 6-31G*	2.41/ 2.01	2.01	2.53/ 5.09/ 2.02	1.97	1.95
	B3LYP/631+G**	3.31/ 2.63	2.07	3.75/ 5.74/ 2.63	2.78	1.96
	MP2/ 3-21G*	3.72/ 2.92	2.03	3.88/ 5.97/ 2.71	2.57	1.82
	MP2/ 6-31G*	4.01/ 2.91	2.06	2.47/ 5.00/ 2.66	2.65	1.86
	HF/LanL2DZ	3.90/2.90	2.06	2.50/ 5.12/ 2.70	2.70	1.87
Bond angle (°)	HF/ 3-21G*	4.56/ 2.95	2.04	2.30/ 4.60/ 2.42	2.85	1.82
	HF/ 6-31G*	171.63/164.38	179.94	112.20	87. 84	177.41
	HF/ 6-31+G**	173.84/162.36	179.94	112.20	87. 82	177.41
	B3LYP/ 3-21G*	174.47/146.79	173.53	107.60	87.82	177.41
	B3LYP/ 6-31G*	176.20/167.80	178.42	111.50	87.82	177.41
	B3LYP/631+G**	168.15/164.73	178.42	111.50	106.35	179.65
	MP2/ 3-21G*	179.99/149.90	178.42	111.50	87.82	178.42
	MP2/ 6-31G*	175.10/147.70	162.50	105.40	96.10	177.65
	MP2/ 6-31+G**	175.90/133.43	179.13	112.50	96.10	179.40
	HF/LanL2DZ	176.20/150.60	178.50	112.20	87.83	178.40

Selected bond distances and bond angles of the reactants (R), transition state (TS) and products (P) are given in Table 3. The TSs for the reaction could be calculated directly from the computational software package. The variations in the bond distances and angles clearly signify the reaction pathway since variation of the Co-Br distance shows how it is transformed to Co-H_2O from Co-Br. The transformation of Co-NH_3 bond to Co-H_2O bond is also perceived in the reaction. The change of Fe-H_2O bond distance showsthe oxidation of iron in $[Fe(H_2O)_6]^{2+}$ to $[Fe(H_2O)]^{3+}$. Similarly, the change of Co-H_2O bond distance also shows its reduction process. Change in the bond length of the TS clearly shows how the Co-Br transforms to the Co-H_2O bond through the Co-Br-Fe formation. It also shows the transformation of Co-NH_3 to Co-H_2O, Co^{III} to Co^{II} and Fe^{II} to Fe^{III}. The bond distances and angles in R, TS and P are well correlated to each other.

5. Conclusions

The rate of the redox reaction between the CoIII complex and Mohr's salt is modulated significantly by the reverse micelles due to encapsulation inside the reverse micellar cavity. Increase of size of water pool decreases the rate. The activation energy of the reaction in aqueous solution calculated theoretically using DFT and the results are in good agreement with the experimental values that support the inner sphere mechanism.

Acknowledgement

The authors thank IIT Kharagpurfor the HR-TEM facility and Dr. S. Chakroborty for helpful discussion regarding the calculation of activation energy by DFT.

References

1. T. Dwars, E. Paetzold, G. Oehme, Reactions in micellar systems, Angew. Chem. Int. Ed. 44(2005) 7174–7199.
2. I. Fernández, J. Pérez-Juste, P. Hervés, Cationic mixed micelles as reaction medium for hydrolysis reactions, J. Solution Chem. 44(2015) 1866–1874.
3. D. Paprocki, A. Madej, D. Koszelewski, A. Brodzka, R. Ostaszewski, Multicomponent reactions accelerated by aqueous

micelles, Front. Chem. 6 (2018) 502.
4. M.A. López-Quintela, C.Tojo, M.C. Blanco, L. García Rio, J.R. Leis, Microemulsion dynamics and reactions in microemulsions, Curr. Opin. Colloid Interface Sci. 9 (2004) 264-278.
5. C. Aubery, C. Solans, S. Prevost, M. Gradzielski, M. Sanchez-Dominguez, Microemulsions as reaction media for the synthesis of mixed oxide nanoparticles: relationships between microemulsion structure, reactivity, and nanoparticle characteristics, Langmuir 29 (2013) 1779–1789.
6. F.M Menger, K.L. Caran, V.A. Seredyuk, Chemical reaction between colliding vesicles, Angew. Chem. Int. Ed. 40 (2001) 3905-3907.
7. J.H. Fendler, Interactions and reactions in reversed micellar systems, Acc. of Chem. Research 9 (1976) 153-161.
8. K. Sawada, M. Ueda, Characteristics of aqueous microenvironments in non-ionic surfactant reverse micelles and their use for enzyme reactions in non-aqueous media, J. Chem. Technol. Biotechnol. 79 (2004) 369-375.
9. A. Patra, T.Q. Luong, R.K. Mitra, M. Havenith, Solvent dynamics in a reverse micellar water-pool: a spectroscopic investigation of DDAB–cyclohexane–water systems, Phys. Chem. Chem. Phys. 15 (2013) 930-939.
10. P.L. Cornejo, R. Jiménez, M. Luisa Moyá, F. Sánchez, J. Burgess, Use of the Brönsted equation in the interpretation of micellar effects in kinetics, Langmuir 12 (1996) 4981- 4986.
11. M. Chen, J. Sun, How understanding the role of an additive can lead to an improved synthetic protocol without an additive: organocatalytic synthesis of chiral diarylmethyl alkynes, Angew. Chem. Int. Ed. 56 (2017) 11966 –11970.
12. B.S. Jursic, A density functional theory study of secondary orbital overlap in endo cycloaddition reactions. an example of a diels−alder reaction between butadiene and cyclopropene, J. Mol. Struct. (Theochem) 499 (2000) 223-231.
13. L. Rodríguez, J. Fermin, R. Añez, J. Angel, A. Chirinos, E. Ocando-Mavarez, Transition-state geometry and activation energy calculation for the retro-ene elimination reaction of propene from diallyl sulfide, Phys. Org. Chem. 15 (2002) 826-830.
14. L.A. Curtiss, K. Raghavachari, P.C. Redfem, J.A. Pople, Assessment of Gaussian-2 and density functional theories for the computation of enthalpies of formation, J. Chem. Phys. 106 (1997) 1063-1079.
15. A.K. Chandra, A. Goursot, Calculation of proton affinities using density functional procedures: a critical study, J. Phys. Chem.100 (1996) 11596-11599.
16. J.E. Lee, W. Choi, B.J. Mhin,Solvent-specific photolytic behavior of octachlorodibenzo-p-dioxin, J. Phys. Chem. A 107 (2003) 2693–2699.
17. F. Colmenero, A.M. Fernández, J. Cobos, V. Timón, Periodic DFT study of the thermodynamic properties and stability of schoepite and metaschoepite mineral phases,ACS Earth Space Chem.3 (2019) 17–28.
18. C.A. White, B.G. Johnson, P.M.W. Gill, M. Head-Gordon, Linear scaling density functional calculations via the continuous fast multipole method, Chem. Phys. Lett. 253 (1996) 268-278.
19. M. Challacombe, E. Schwegler, Linear scaling computation of the Fock matrix, J. Chem. Phys.106 (1997) 5526-5536.
20. C. Møller, M.S. Plesset, Note on an approximation treatment for many-electron systems, Phys. Rev. 46 (1934) 618-622.
21. A.D. Becke, Density-functional exchange-energy approximation with correct asymptotic behavior, Phys. Rev. A 38 (1988) 3098-3100.
22. C. Lee, W. Yang, R.G. Parr, Development of the Colle-Salvetti correlation-energy formula into a functional of the electron density, Phys. Rev. B 37 (1988) 785-789.
23. M.M. Francl, W.J. Pietro, W.J. Hehre, J.S. Binkley, M.S. Gordon, D.J. De Frees, J.A. Pople, Self-consistent molecular orbital methods. XXIII. A polarization-type basis set for second-row elements, J. Chem. Phys.77 (1982) 3654-3665.
24. F.A. Posey, H. Taube, The mechanisms of substitution reactions of octahedral complexes: the induced aquation of the halogenopentamminecobaltic ions by metal cations, J. Am. Chem. Soc. 79 (1957) 255-262.